Supporting Information

Self-Regenerative Noble Metal Catalysts Supported on High-Entropy Oxides

Hao Chen,[a] Yifan Sun,*[b] Shize Yang,[†c] Hui Wang,[d] Wojciech Dmowski,[d] Takeshi Egami,[def] Sheng Dai*[ab]

[a] Department of Chemistry, The University of Tennessee, Knoxville, Tennessee 37996, USA. E-mail: dais@ornl.gov.

[b] Chemical Sciences Division, Oak Ridge National Laboratory, Oak Ridge, Tennessee 37831, USA. E-mail: suny@ornl.gov.

[c] Center for Functional Nanomaterials, Brookhaven National Laboratory, Upton, New York 11973, USA

[d] Department of Materials Science and Engineering, The University of Tennessee, Knoxville, Tennessee 37996, USA

[e] Department of Physics and Astronomy, The University of Tennessee, Knoxville, Tennessee 37996, USA

[f] Materials Science and Technology Division, Oak Ridge National Laboratory, Oak Ridge, Tennessee 37831, USA

[†] Current Address: Eyring Materials Center, Arizona State University, Tempe, Arizona 85287, USA

Experimental Details

Materials. Magnesium oxide (MgO, 98%, -100 mesh), copper (II) oxide (CuO, ≥ 99%) and zinc oxide (ZnO, 98%) were purchased from ACROS Organics. Cobalt (II) oxide (CoO, 95%) and nickel (II) oxide (NiO, 99.0%) were purchased from Alfa Aesar. Gold (III) oxide hydrate ($Au_2O_3 \cdot xH_2O$), palladium (II) oxide (PdO, 99.97% trace metals basis) and ruthenium (IV) oxide (RuO_2, 99.9% trace metals basis) were purchased from Sigma Aldrich. All chemicals were used as received without further purification.

Synthesis of Au-HEOs. Solid-state synthesis of HEOs and Au-HEOs are modified based on the previous report.[1] 5 mmol of NiO (374 mg), MgO (202 mg), CuO (398 mg), ZnO (407 mg) and CoO (375 mg), together with 22 mg Au_2O_3 corresponding to 1 wt% Au loading, were thoroughly grinded. Au-HEO-900 was prepared by calcinating the mixed powders to 900 °C in air for 4 h, and naturally cooling down to room temperature. Similar synthetic protocols were adopted for other 1 wt% HEO-supported noble metal samples. Au-HEO-700 was obtained by calcinating the Au-HEO-900 sample at 700 °C in air for 4 h, and naturally cooling down to room temperature.

Characterization. Powder X-ray diffraction (XRD) patterns were collected using a PANalytical Empyrean X-ray diffractometer equipped with Cu Kα radiation, with the operating voltage of 45 kV and current of 40 mA. Simulated XRD patterns were generated using the CrystalMaker/CrystalDiffract software package. High-angle annular dark-field scanning transmission electron microscopy (HAAD-STEM) images and energy dispersive X-ray spectroscopy (EDS) data with element maps were collected on a FEI Talos 200F microscope at 200 kV. Inductively coupled plasma-atomic emission spectroscopy (ICP-AES) was performed using an Optima 2100 DV spectrometer (PerkinElmer Corporation). X-ray photoelectron spectroscopy (XPS) measurements were performed with a PHI 3056 spectrometer equipped with an Al anode source operated at 15 kV with an applied power of 350 W and a pass energy of 93.5 eV. Samples were mounted on foil, and peaks were charge referenced to the CH_x peak in the carbon 1s spectra at 284.8 eV. The high-energy x-rays (100 keV, λ = 0.1235 Å) diffraction experiments on the powder samples were performed at the 6-ID beamlines of the Advanced Photon Source (APS) at Argonne National Laboratory. Two-dimensional (2D) detectors, placed ~40 cm behind the sample, with 2048 × 2048 pixels and 200μm × 200μm pixel size were used to collect data. Calibration was performed using the CeO_2 standard samples from National Institute of Standards and Technology (NIST). 2D diffraction data were processed by FIT2D.[2] GSAS-II was used to obtain the structure information.[3]

Catalytic measurements. CO oxidation was performed using the Altamira Instruments system with the catalysts loaded in a fixed-bed reactor (U-type quartz tube) with inner diameter of 4 mm at atmospheric pressure. 40 mg of the Au-HEO catalyst was loaded in the reactor with quartz wool as support. The feed gas of 1% CO balanced with dry air passed though the catalyst bed at a flow rate of 12 mL min^{-1}, corresponding to a gas hourly space velocity of 18000 mL $(h\ g)^{-1}$. The reactants and products were analyzed using a Buck MG#5 gas chromatograph (GC) equipped with a thermal conductivity detector and a ShinCarbon ST column.

Supplementary Tables

Table S1 Noble metal percentages supported on HEOs quantified by ICP-AES.

Sample	Noble Metal Element	Percentage / wt%
Au-HEO-900	Au	1.1
Au-HEO-700	Au	0.9
Pd-HEO-900	Pd	1.8
Ru-HEO-900	Ru	1.3

Table S2 GSAS-II Rietveld refinement results.

Sample	Lattice Parameter of FCC Structure / Å	FCC Phase Percentage / %	R_{wp} / %
MgO	4.214	100	6.7
HEO	4.208	84.7	9.7
Au-HEO-900	4.219	100	10.6

Supplementary Figures

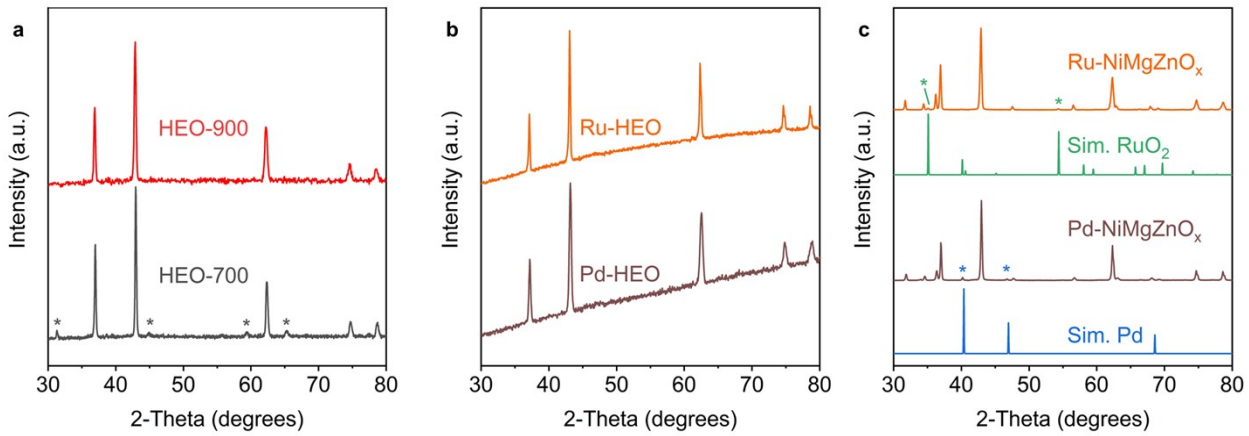

Fig. S1 Powder XRD patterns of (a) HEO prepared at 900 °C (HEO-900) and annealed at 700 °C (HEO-700), (b) 1 wt% Pd and Ru supported on HEOs calcinated at 900 °C, and (c) 1 wt% Pd and Ru supported on ternary oxides ($NiMgZnO_x$) calcinated at 900 °C, with emerging impurity peaks highlighted with asterisk symbols. Simulated XRD patterns for RuO_2 and Pd are listed for comparison.[4,5]

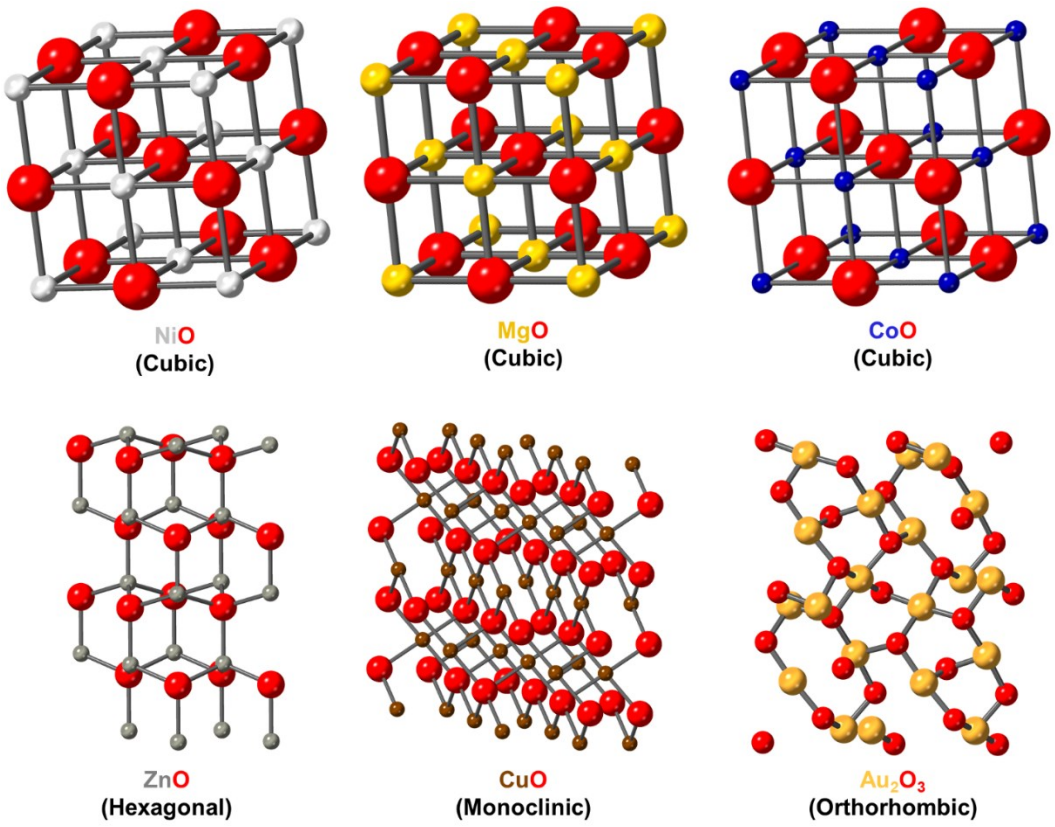

Fig. S2 Crystal structures of NiO, MgO, CoO, ZnO, CuO and Au_2O_3.[6–9] One unit cell is exhibited for NiO, MgO, CoO, and Au_2O_3, while eight are included for ZnO and CuO for a better illustration.

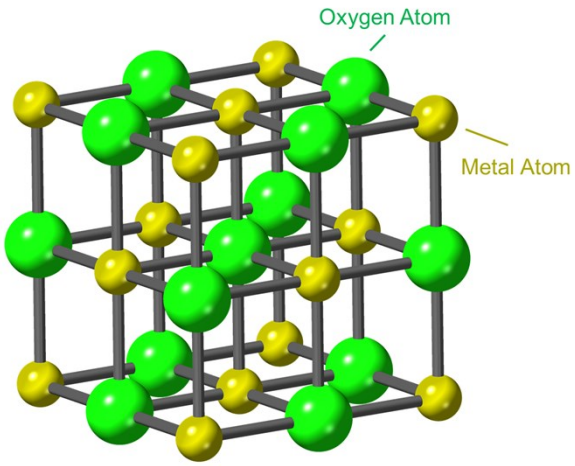

Fig. S3 Schematic showing the positions of metal (dark yellow) and oxygen (green) atoms in the cubic lattice of Au-HEO-900 for GSAS-II refinement.

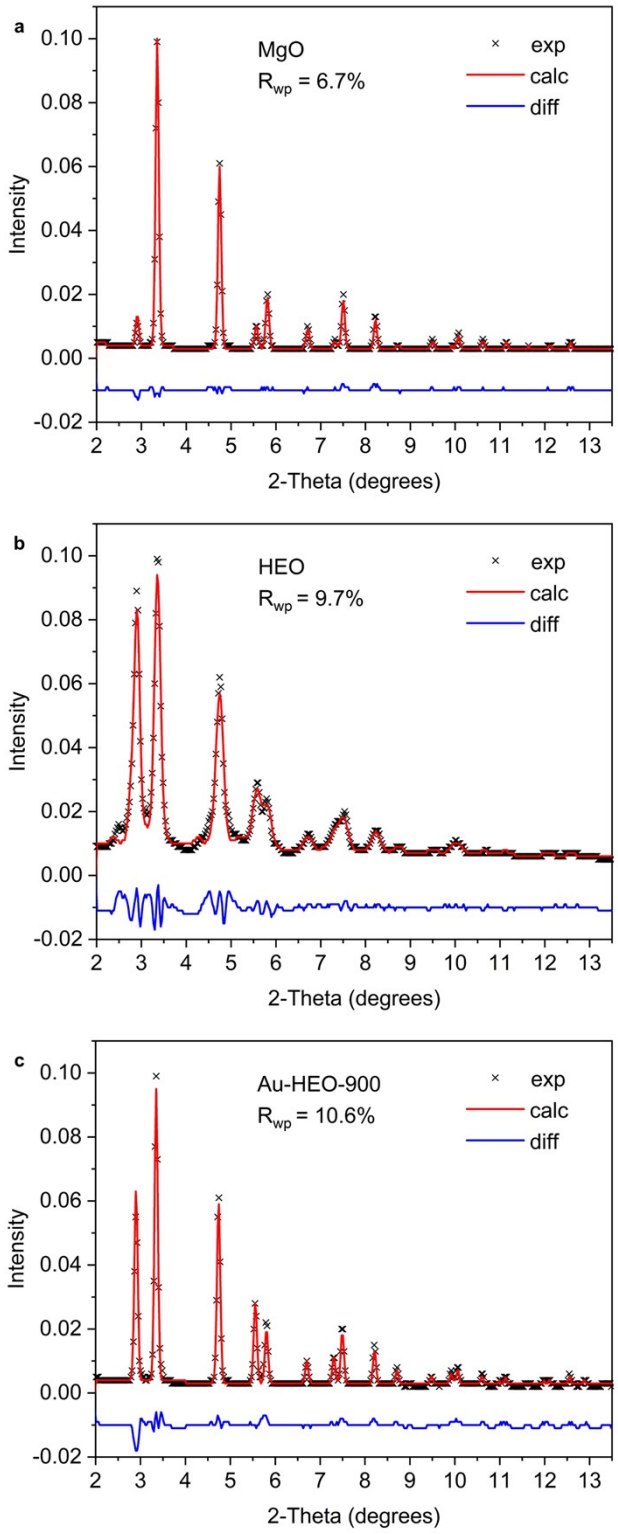

Fig. S4 Rietveld refinements for (a) MgO, (b) HEO, and (c) Au-HEO-900 by GSAS-II.

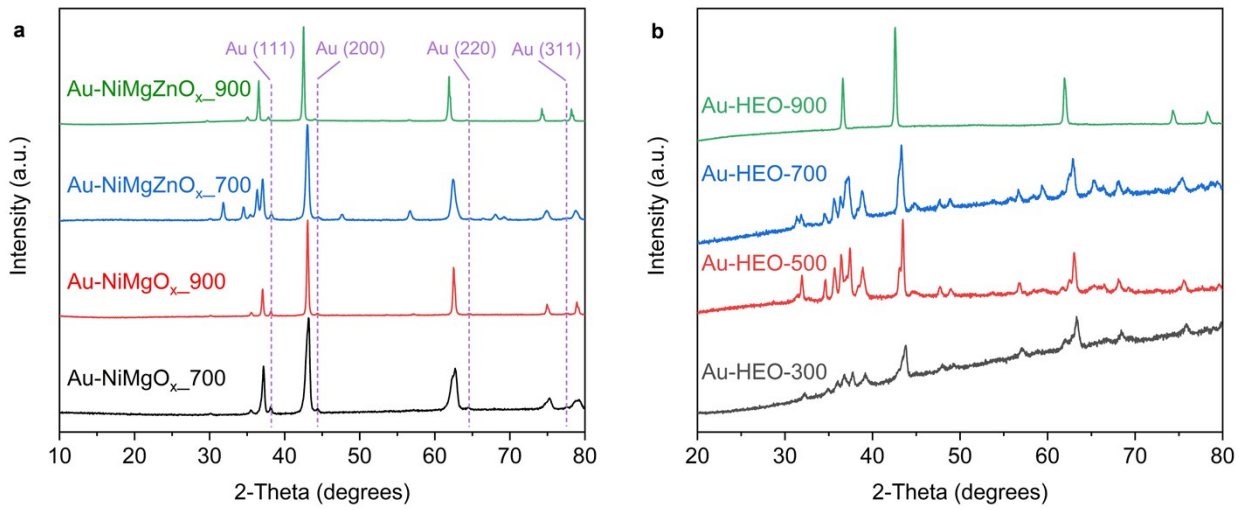

Fig. S5 (a) Powder XRD patterns of Au supported on binary ($NiMgO_x$) and ternary ($NiMgZnO_x$) oxides at 700 and 900 °C, respectively, where multiple impurity phases appear. Diffraction peaks corresponding to Au are highlighted by the purple dotted lines. (b) Powder XRD patterns of Au-HEO synthesized via annealing at different temperatures in air.

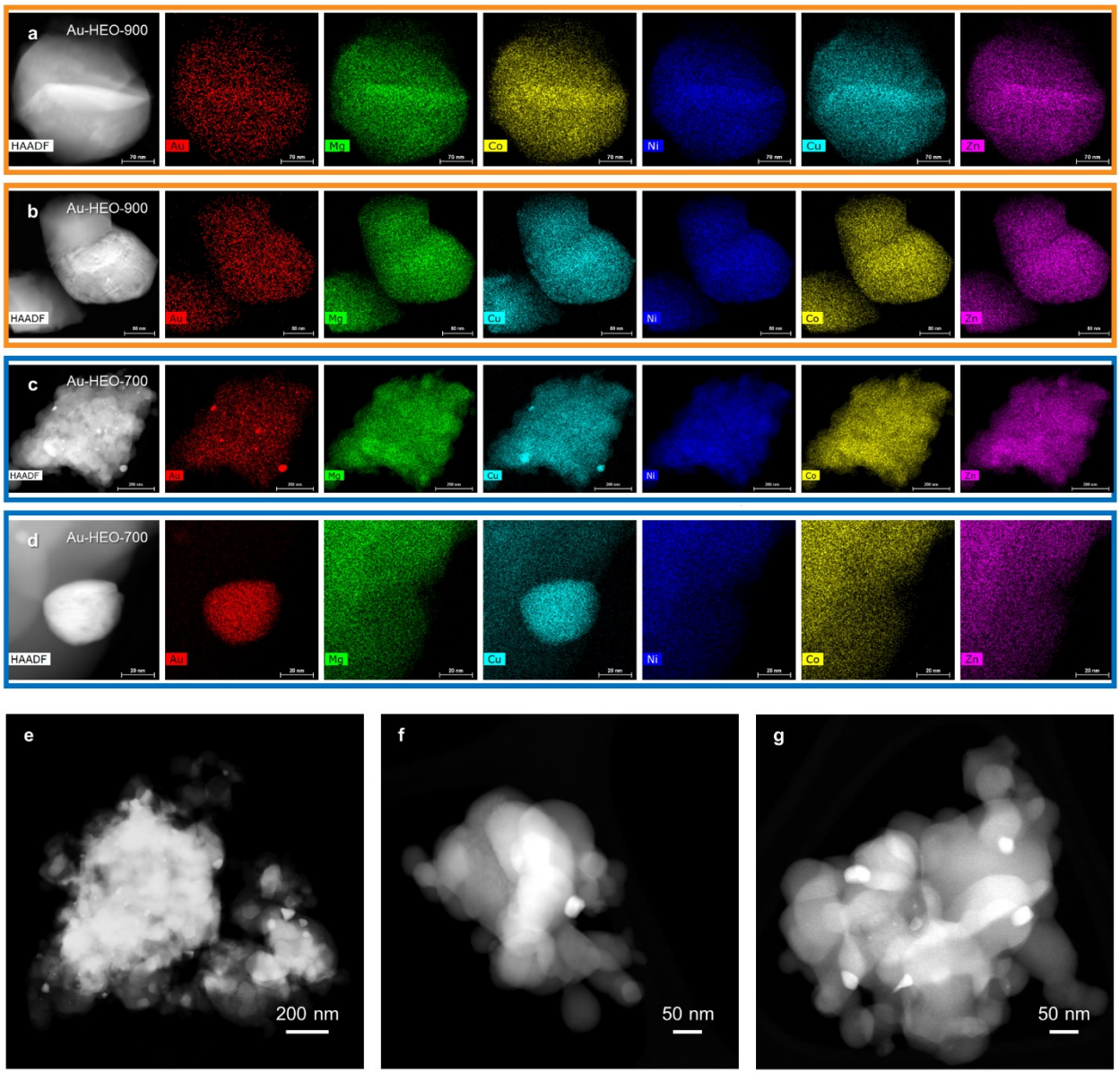

Fig. S6 HAADF-STEM images with EDS elemental maps of (a,b) Au-HEO-900 and (c,d) Au-HEO-700. (e-f) Additional HAADF-STEM images showing the formation of the exsoluted Au nanoparticles that exhibit higher contrast in Au-HEO-700.

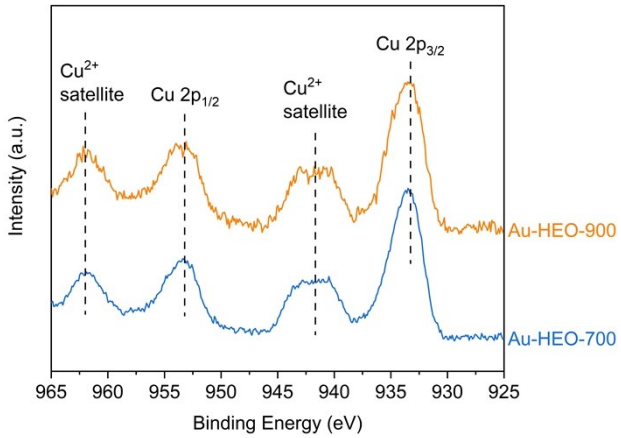

Fig. S7 XPS spectra for Au-HEO-700 and Au-HEO-900 of the Cu 2p region, showing the existence of Cu^{2+} in both cases.

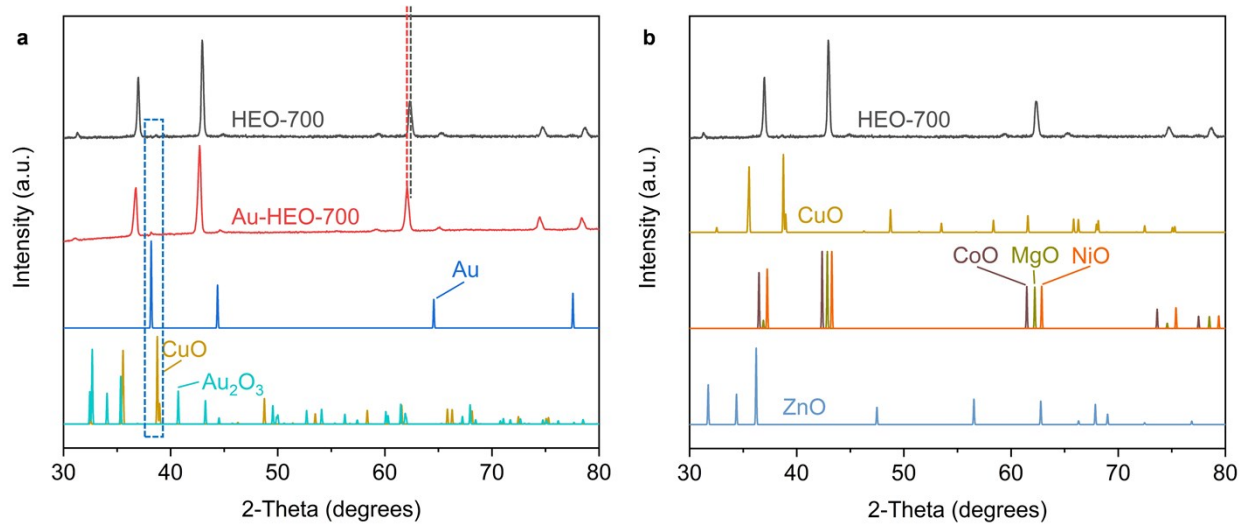

Fig. S8 (a) Powder XRD patterns of HEO-700 and Au-HEO-700 with simulated reference patterns of Au, CuO and Au_2O_3, where the impurity peak of Au-HEO-700 around 38° is attributed to Au, rather than CuO or Au_2O_3, based on the comparison highlighted by the dotted blue lines.[5] The diffraction peaks of Au-HEO-700 are shifted towards the lower angles compared with the ones from HEO-700, indicating lattice expansion caused by residual Au cations in the HEO lattice. (b) Powder XRD pattern of HEO-700 with simulated ones of CuO, CoO, MgO, NiO and ZnO.[6–9]

References

[1] Rost, C. M.; Sachet, E.; Borman, T.; Moballegh, A.; Dickey, E. C.; Hou, D.; Jones, L. J.; Curtarolo, S.; Maria, J.-P. Entropy-Stabilized Oxides. *Nat. Commun.* **2015**, *6*, 8485.

[2] Hammersley, A. P.; Svensson, S. O.; Thompson, A.; Graafsma, H.; Kvick, A.; Moy, J. P. Calibration and Correction of Spatial Distortions in 2D Detector Systems. *Rev. Sci. Instr., (SRI-94)*, **1995**, *66*, 2729–2733.

[3] Toby, B. H.; Von Dreele, R. B. GSAS-II: The Genesis of a Modern Open-Source All Purpose Crystallography Software Package. *J. Appl. Crystallogr.* **2013**, *46*, 544–549.

[4] Takeda, T.; Nagata, M.; Kobayashi, H.; Kanno, R.; Kawamoto, Y.; Takano, M.; Kamiyama, T.; Izumi, F.; Sleight, A. W. High-Pressure Synthesis, Crystal Structure, and Metal–Semiconductor Transitions in the $Tl_2Ru_2O_{7-\delta}$ Pyrochlore. *J. Solid State Chem.* **1998**, *140*, 182–193.

[5] Davey, W. P. Precision Measurements of the Lattice Constants of Twelve Common Metals. *Phys. Rev. B.* **1925**, *25*, 753–761.

[6] Sasaki, S.; Fujino, K.; Takéuchi, Y. X-Ray Determination of Electron-Density Distributions in Oxides, MgO, MnO, CoO, and NiO, and Atomic Scattering Factors of their Constituent Atoms. *Proc. Japan Acad. Ser. B* **1979**, *55*, 43–48.

[7] Schulz, H.; Thiemann, K. H. Structure Parameters and Polarity of the Wurtzite Type Compounds Sic—2H and ZnO. *Solid State Commun.* **1979**, *32*, 783–785.

[8] Åsbrink, S.; Norrby, L.-J. A Refinement of the Crystal Structure of Copper(II) Oxide with a Discussion of Some Exceptional e.s.d.'s. *Acta Cryst. B* **1970**, *26*, 8–15.

[9] Jones, P. G.; Rumpel, H.; Schwarzmann, E.; Sheldrick, G. M.; Paulus, H. Gold(III) oxide. *Acta Cryst. B* **1979**, *35*, 1435–1437.